Ultra-wideband microwave photonic phase shifter with a 360° tunable phase shift based on an erbium-ytterbium co-doped linearly chirped FBG

Weilin Liu and Jianping Yao*

Microwave Photonics Research Laboratory, School of Electrical Engineering and Computer Science, University of Ottawa, Ottawa, Ontario K1N 6N5, Canada

**Corresponding author: jpyao@eecs.uottawa.ca*

Received November 20, 2013; revised December 28, 2013; accepted December 31, 2013; posted January 3, 2014 (Doc. ID 201612); published February 10, 2014

A simple photonic approach to implementing an ultra-wideband microwave phase shifter based on an erbium–ytterbium (Er/Yb) co-doped linearly chirped fiber Bragg grating (LCFBG) is proposed and experimentally demonstrated. The LCFBG is designed to have a constant magnitude response over a reflection band, and a phase response that is linear and nonlinear in two sections in the reflection band. When an optical single-sideband with carrier (OSSB + C) signal is sent to the LCFBG, by locating the optical carrier at the section corresponding to the nonlinear phase response and the sideband at the section corresponding to the linear phase response, a phase shift is introduced to the optical carrier, which is then translated to the microwave signal by beating the optical carrier and the sideband at a photodetector. The tuning of the phase shift is realized by optically pumping the Er/Yb co-doped LCFBG by a 980-nm laser diode. The proposed ultra-wideband microwave photonic phase shifter is experimentally demonstrated. A phase shifter with a full 360° phase shift with a bandwidth from 10 to 40 GHz is experimentally demonstrated.

OCIS codes: (050.5080) Phase shift; (060.3735) Fiber Bragg gratings; (350.4010) Microwaves; (060.5625) Radio frequency photonics.

http://dx.doi.org/10.1364/OL.39.000922

Microwave phase shifters (MPSs) are important devices in microwave systems for applications such as phased-array beamforming for wireless communications and radar systems [1–4]. An MPS can be implemented based on a semiconductor dielectric integrated circuit [5] or a ferrite-ferroelectric waveguide structure [6]. A semiconductor-based MPS has a high response speed, but the power-handling capacity is poor, and the insertion losses are high [5]. On the contrary, a ferrite-based MPS has better power-handling capacity, and the losses are smaller, but the response speed is limited, and the size is usually large [6]. To implement an MPS with a large bandwidth, small size, and high response speed, a solution is to use photonic techniques. In the past few years, numerous photonic-assisted MPSs were proposed [7–11]. In [7], an MPS with a phase shift of 180° was realized based on cross-phase modulation (XPM) in a nonlinear loop mirror, in which the phase of the optical carrier of an optical single-sideband with carrier (OSSB + C) signal is modulated through XPM [7], and the beating of the optical carrier and the sideband generates a microwave signal with the phase shift directly translated to the microwave signal. In [8], an MPS with a phase shift of 135° based on wavelength conversion in a DFB laser was proposed. The fundamental principle of the technique is to introduce a phase shift to the new wavelength during the wavelength conversion, and the phase shift is tunable by controlling the injection current to the DFB laser. Other techniques to implement an MPS include the use of slow- and fast-light effects in a semiconductor optical amplifier (SOA) [9] or in a tilted fiber Bragg grating [10], and the use of stimulated Brillouin scattering (SBS) effect in an optical fiber [11]. The approaches reported in [7,8,10] have the limitation to provide a full 360° phase shift. Although the approach in [9] can achieve a full 360° phase shift, the system is complicated due to the use of multiple SOAs. The SBS-assisted MPS can also provide a full 360° phase shift [11], but to trigger the SBS, a high-power optical pump source is needed, and the optical fiber is usually long. In addition, the SBS effect is sensitive to environmental changes, which may affect the stability of the system.

Recently, we proposed a technique to implement an MPS with a full 360° phase shift using a polarization-maintaining fiber Bragg grating (PM-FBG) [12]. In the proposed system, an OSSB + C signal was sent to a PM-FBG, which has two spectrally separated transmission notches along the fast and the slow axes. By locating the optical carrier along the fast axis at the transmission notch, the optical carrier in the OSSB + C signal was removed. At the output of the PM-FBG, two orthogonally polarized optical signals, one with the optical carrier and the sideband, the other with only the sideband, are obtained. The two orthogonal signals are then sent through a variable retardation plate (VRP) to a polarizer and then detected by a photodetector (PD). By controlling the VRP to introduce a tunable phase difference between the two orthogonally polarized signals, a microwave signal with a tunable phase shift was generated. Although a working bandwidth from 10 to 40 GHz was achieved, the phase tuning speed of the proposed system is slow due to the use of a VRP.

In this Letter, a simple photonic approach to implementing an ultra-wideband MPS with a high tuning speed based on an erbium-ytterbium (Er/Yb) co-doped linearly chirped fiber Bragg grating (LCFBG) is proposed and experimentally demonstrated. In the proposed system, as shown in Fig. 1, an OSSB + C signal generated using a Mach–Zehnder modulator (MZM) followed by an optical notch filter to remove the upper sideband is sent to an Er/Yb co-doped LCFBG via an optical circulator. The LCFBG is custom-made with a flat magnitude response

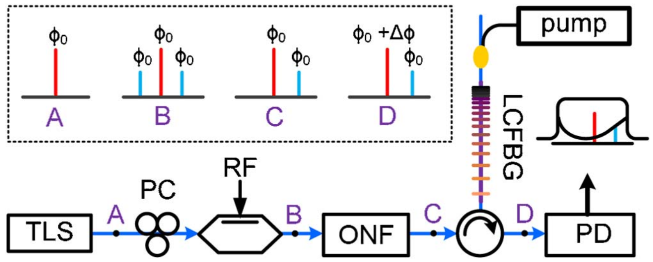

Fig. 1. Schematic of the proposed ultra-wideband 360° microwave photonic phase shifter. TLS, tunable laser source; PC, polarization controller; RF, radio frequency; ONF, optical notch filter; PD, photodetector; LCFBG, linearly chirped fiber Bragg grating.

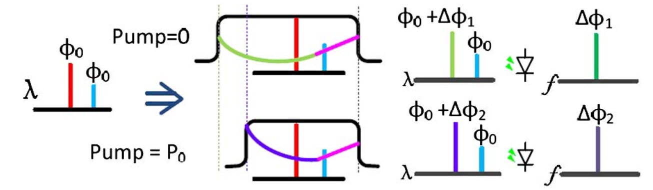

Fig. 2. Principle of the proposed phase shifter based on an Er/Yb co-doped LCFBG.

in the reflection band. The phase response in the reflection band is divided into two sections, with one section having a nonlinear phase response, and the other section having a linear phase response. When the Er/Yb co-doped LCFBG is optically pumped from the end of the section with a nonlinear phase response by a 980-nm laser diode (LD), the nonlinear phase response will be changed accordingly due to the pump-induced refractive index change in the Er/Yb co-doped fiber [13]. By locating the optical carrier and the sideband in the nonlinear and linear sections of the phase response, respectively, the phase of the optical carrier can be tuned by changing the pump power, but the phase of the optical sideband is not changed. In this way, the phase change of the optical carrier can be translated to the generated microwave signal by beating the optical carrier and the sideband at a PD. The key advantage of using optical pumping to tune the phase response of the LCFBG over external thermal [14] or mechanical tuning [15] is that the phase response can be tuned at a much higher speed and controlled remotely. In addition, the undesirable birefringence effects existing in the mechanical tuning technique can also be avoided.

The key component in the proposed system is the LCFBG, which is inscribed in an Er/Yb co-doped optical fiber. The refractive index modulation $\Delta n(z)$ of such an LCFBG can be written as

$$\Delta n(z) = \mathrm{Re}\left\{\frac{[n_m(z)+\delta(z)]}{2}\exp\left\{j\left[\frac{2\pi z}{\Lambda(z)}+\phi_g(z)\right]\right\}\right\}, \quad (1)$$

where z is the position along the grating, $n_m(z)$ denotes the maximum index modulation, $\delta(z)$ is the index change in the desired area with linear phase response, and $\Lambda(z)$ and $\phi_g(z)$ are the central pitch and the local phase of the single-channel seed grating, respectively. The designed LCFBG can be fabricated in a hydrogen-loaded Er/Yb co-doped fiber with the conventional phase-mask-based FBG writing technique using a continuous-wave UV light at 244 nm [16]. To obtain a section with a linear phase response in the LCFBG, $\delta(z)$ needs to be controlled such that the desired linear phase response section has a strong reflection, which is achieved by enhancing the UV exposure implemented through multiple scans. The section with a nonlinear phase response in the LCFBG has a weak reflection, and the nonlinear phase response can be changed by optically pumping the section. When the LCFBG is optically pumped from the blue end, i.e., the end with the shortest period, the temperature at the blue end would increase, which would force the blue end to move to the red end and therefore shorten the reflection band as a consequence of the increase in the core refractive index, as shown in Fig. 2. Thus, the phase response corresponding to the section with a nonlinear phase is changed due to the optical pumping. However, the thermal effect induced by the optical pump along the LCFBG is not uniform. At the red end of the LCFBG, due to the strong absorption of the Er/Yb co-doped fiber, the thermally induced refractive index change is small and negligible. Thus the section with a linear phase response will experience negligible phase change when the LCFBG is optically pumped from the blue end. By tuning the injection current to the pumping LD, the nonlinear phase response of the LCFBG can be continuously tuned.

An experiment based on the setup shown in Fig. 1 is implemented. A linearly polarized OSSB + C modulated signal generated using an MZM followed by an optical notch filter to remove the upper sideband is sent to the Er/Yb co-doped LCFBG. The notch filter is a WaveShaper (Finisar, WaveShaper 4000S) with a bandwidth of a 50 GHz and a notch rejection of 50 dB. The optical carrier is controlled to locate at the section with a nonlinear phase response. To ensure a large frequency tunable range, the carrier is placed close to the border to the section with a linear phase response. In the experiment, the wavelength of the optical carrier is 1554.64 nm. By pumping the Er/Yb co-doped LCFBG, the nonlinear phase response will change accordingly; thus the optical carrier is reflected back with a phase change relative to the optical sideband. The spectrum of the OSSB + C signal with a modulated microwave signal at 30 GHz and the magnitude spectral response of the Er/Yb co-doped LCFBG with different pumping powers are shown in Fig. 3(a); the corresponding phase response is shown in Fig. 3(b). The magnitude response and the phase response of the Er/Yb co-doped LCFBG are measured by an optical vector analyzer (OVA, Luna Technologies). Note that during the fabrication of the LCFBG, it is controlled that the section with a linear phase response has a strong reflection and that with a nonlinear phase response has a weak reflection. As can be seen from Fig. 3(a), the reflection in the section with a linear phase response is about 0.7 dB greater than that in the section with a nonlinear phase response.

In the proposed system, the phase difference between the optical carrier and the sideband is controlled by tuning the pump power, which is a 980-nm LD. By beating the optical carrier and the sideband, a microwave signal, with its phase tunable by tuning the pump power is

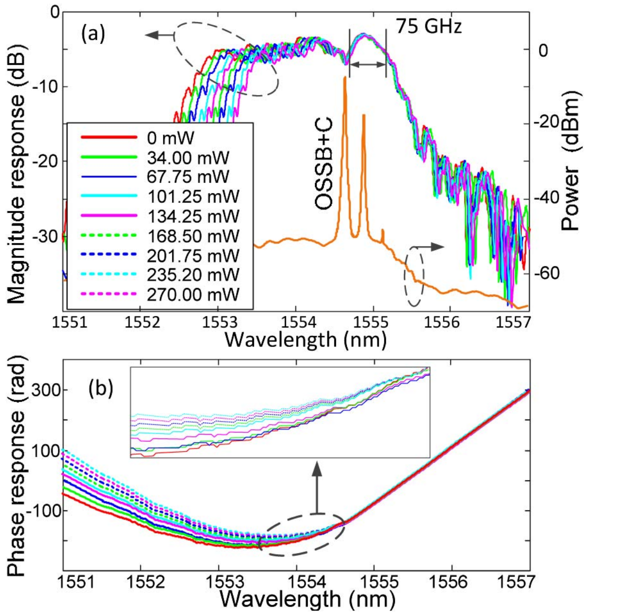

Fig. 3. (a) Reflection spectrum of the LCFBG when pumped with different pumping powers. The spectrum of the OSSB + C signal is also shown. (b) Corresponding phase response of the LCFBG.

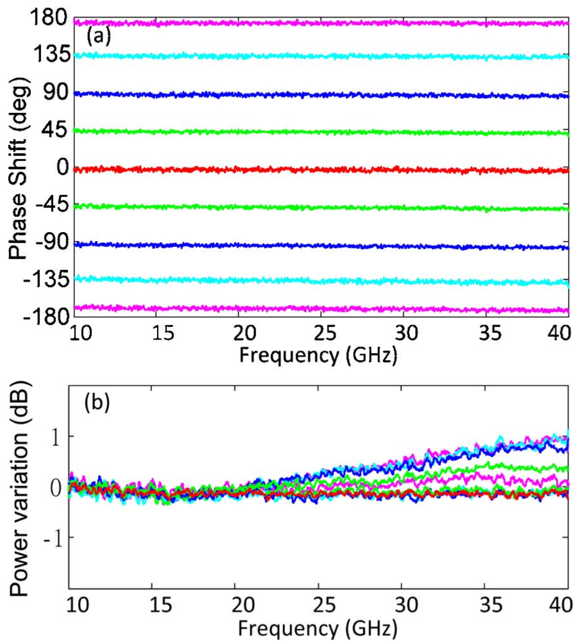

Fig. 4. (a) Experimentally generated phase shift over a frequency range of 10 to 40 GHz. (b) Relative power change of the phase-shifted microwave signal for different phase shifts.

obtained at the output of the PD. Figure 4(a) shows the phase shift measured using a vector network analyzer (VNA, Agilent E8364A). As can be seen, a tunable phase shift from −180° to 180° over a frequency range of 10 to 40 GHz is achieved. The lowest frequency is limited by the distance from the location of the optical carrier to the border of the section with a linear phase response of the Er/Yb co-doped LCFBG. The highest frequency is limited by the bandwidth of the MZM and the PD. If an MZM and a PD with a wider bandwidth are used in the experiment, the frequency range should be extended up to 75 GHz, which is then limited by the width of the section with a linear phase response of the Er/Yb co-doped LCFBG.

For an ideal phase shifter, it is expected that the output power is not phase dependent over the bandwidth. To study the power dependence for the proposed phase shifter, the microwave power for different phase shifts at different pumping power levels is also measured by the VNA, with the results shown in Fig. 4(b). As can be seen, the microwave powers for different phase shifts over the bandwidth from 10 to 40 GHz are maintained almost constant. The output power variation for the entire 360° phase shift range is within 1 dB.

In conclusion, we have proposed and experimentally demonstrated a novel photonic approach to implementing an ultra-wideband MPS based on an Er/Yb co-doped LCFBG. The key significance of the proposed technique is the use of an optically pumped Er/Yb co-doped LCFBG, which ensures the realization of an ultra-wideband MPS with a tunable phase shift over a full 360° range. The proposed technique was experimentally demonstrated. A phase shifter with a full 360° phase shift with a bandwidth from 10 to 40 GHz was experimentally demonstrated.

This work was supported by the Natural Sciences and Engineering Research Council of Canada (NSERC) through the Strategic Project Grants program.

References

1. A. Yamagashi, M. Ishikawa, T. Tsukahara, and S. Date, *CICC Digest of Technical Papers* (1995), p. 319.
2. J.-L. Kuo, Y.-F. Lu, T.-Y. Huang, Y.-L. Chang, Y.-K. Hsieh, P.-J. Peng, I.-C. Chang, T.-C. Tsai, K.-Y. Kao, W.-H. Hsiung, J. Wang, Y. A. Hsu, K.-Y. Lin, H.-C. Lu, Y.-C. Lin, L.-H. Lu, T.-W. Huang, R.-B. Wu, and H. Wang, IEEE Trans. Microwave Theory Tech. **60**, 743 (2012).
3. J. F. Coward, T. K. Yee, C. H. Chalfant, and P. H. Chang, J. Lightwave Technol. **11**, 2201 (1993).
4. M. Attygalle and D. Stepanov, Opt. Express **20**, 18025 (2012).
5. H. Jacobs and M. M. Chrepta, IEEE Trans. Microwave Theory Tech. **22**, 411 (1974).
6. A. B. Ustinov, G. Srinivasan, and B. A. Kalinikos, Appl. Phys. Lett. **90**, 031913 (2007).
7. Y. Dong, H. He, and W. Hu, Opt. Lett. **32**, 745 (2007).
8. M. R. Fisher and S. L. Chuang, IEEE Photon. Technol. Lett. **18**, 1714 (2006).
9. W. Xue, S. Sales, J. Capmany, and J. Mørk, Opt. Lett. **34**, 929 (2009).
10. H. Shahoei and J. P. Yao, Opt. Express **20**, 14009 (2012).
11. A. Loayssa and F. J. Lahoz, IEEE Photon. Technol. Lett. **18**, 208 (2006).
12. W. Liu, W. Li, and J. P. Yao, IEEE Photon. Technol. Lett. **25**, 1107 (2013).
13. M. K. Davis, M. J. Digonnet, and R. Pantell, J. Lightwave Technol. **16**, 1013 (2003).
14. J. Lauzon, S. Thibault, J. Martin, and F. Ouellette, Opt. Lett. **19**, 2027 (1994).
15. Y. Liu, J. P. Yao, X. Dong, and J. Yang, Opt. Eng. **41**, 740 (2002).
16. M. Bernier, Y. Sheng, and R. Vallée, Opt. Express **17**, 3285 (2009).